

Article

Not peer-reviewed version

Research on Aging Characteristics and Interfacial Adhesion Performance of Polyurethane-Modified Asphalt

[Meng Wang](#) , Jixian Li , Lu Chen , [Changyun Shi](#) ^{*} , [Jinguo Ge](#)

Posted Date: 15 September 2025

doi: 10.20944/preprints202509.1154.v1

Keywords: pavement engineering; polyurethane-modified asphalt; rheological properties; molecular simulation; work of adhesion



Preprints.org is a free multidisciplinary platform providing preprint service that is dedicated to making early versions of research outputs permanently available and citable. Preprints posted at Preprints.org appear in Web of Science, Crossref, Google Scholar, Scilit, Europe PMC.

Copyright: This open access article is published under a Creative Commons CC BY 4.0 license, which permit the free download, distribution, and reuse, provided that the author and preprint are cited in any reuse.

Article

Research on Aging Characteristics and Interfacial Adhesion Performance of Polyurethane-Modified Asphalt

Meng Wang ^{1,2}, Jixian Li ^{1,2}, Lu Chen ¹, Changyun Shi ^{3,4,*} and Jinguo Ge ⁵

¹ School of Civil Engineering and Architecture, Jiaxing Nanhu University, Jiaxing, Zhejiang, China

² G60 STI Valley Industry & Innovation Institute, Jiaxing University, Jiaxing, Zhejiang, China

³ School of Civil Engineering, University of South China, Hengyang, Hunan, China

⁴ Hunan Provincial Key Laboratory of High-Performance Special Concrete, University of South China, Hengyang, Hunan, China

⁵ College of Transportation Engineering, Changsha University of Science and Technology, Changsha, Hunan, China

* Correspondence: 2024001056@usc.edu.cn

Abstract

Polyurethane (PU) owing to its superior physicochemical properties, is considered an ideal modifier for asphalt. To enhance the mechanical performance and service durability of asphalt pavements, PU-modified asphalts with varying dosages were prepared and systematically evaluated through a combination of laboratory experiments and molecular dynamics simulations. Aging tests, rheological and thermodynamic analyses, mechanical property evaluations, and asphalt–aggregate interfacial adhesion energy calculations were conducted to elucidate the modification mechanism, aging resistance, and interfacial behavior. The results showed that PU incorporation markedly improved rutting resistance at high temperatures and flexibility at low temperatures, thereby enhancing the load-bearing capacity of asphalt. Under ultraviolet and long-term aging conditions, PU-modified asphalts exhibited significantly lower performance degradation than base asphalt, highlighting their superior anti-aging properties. At the molecular level, PU adsorbed light fractions and formed a cross-linked network, reducing the free volume fraction while enhancing mechanical strength and deformation resistance. Additionally, PU substantially increased asphalt–aggregate adhesion energy, strengthening interfacial bonding. However, excessive PU content led to molecular aggregation and partial phase separation, compromising system stability. These findings provide theoretical insights and practical guidance for the optimal design and engineering application of PU-modified asphalt.

Keywords: pavement engineering; polyurethane-modified asphalt; rheological properties; molecular simulation; work of adhesion

1. Introduction

Asphalt as a vital material for road construction, has become the primary choice for pavement engineering due to its ease of construction, cost-effectiveness, and convenient maintenance [1,2]. The performance of asphalt directly determines the service quality of pavements. However, with increasing traffic loads and the impacts of climate change, conventional asphalt materials could no longer fully meet pavement performance requirements. Asphalt modification has therefore emerged as an effective approach to enhance asphalt properties [3]. By incorporating various types of polymers, inorganic materials, or other functional additives, modification technologies could improve the mechanical properties, aging resistance, and adhesion to aggregates [4]. Traditional

modification methods, such as the addition of polymers, rubber, or asphalt modifiers, have improved asphalt performance to some extent, but still face limitations related to the selection and stability of modifiers [5]. In recent years, PU owing to its excellent mechanical performance, chemical stability, and weather resistance, has attracted increasing attention as a novel modifier in the field of asphalt modification [6]. As a polymeric material with a distinctive chemical structure, PU could effectively enhance asphalt performance, particularly in terms of rheological properties, anti-aging behavior, and interfacial adhesion [4,7–9]. Compared with conventional modifiers, PU was capable of forming cross-linked networks and strong intermolecular interactions, which significantly improve asphalt's cracking resistance and moisture damage resistance, thereby greatly extending the service life of pavements [10–12].

As the fifth largest polymer material worldwide, PU is a promising polymer with excellent mechanical properties, good weather resistance, and strong adhesion [13,14]. Numerous studies have investigated various aspects of PU-modified asphalt, including its preparation process, rheological behavior, and microstructural characteristics. For example, Jin et al. [15] prepared PU-rock asphalt (RA) composite-modified asphalt and found that PU enhanced the low-temperature performance of base asphalt, while proposing an optimal dosage based on compatibility indices. Wang et al. [16] developed a dynamic cross-linking synthesis method for PU-modified asphalt and demonstrated that the flexibility of the material could be tuned by adjusting the NCO/OH ratio. Another notable advantage of PU was its superior aging resistance [17,18], which helps maintain asphalt performance and extend its service life [19–21]. Despite its promise and widespread application in asphalt modification, research on PU-modified asphalt still exhibits several limitations. Most existing studies have focused on macroscopic performance evaluations, such as rheological properties, mechanical strength, and aging resistance. Although these investigations provide valuable theoretical support for the application of PU-modified asphalt, they have not sufficiently explored the underlying molecular mechanisms and interfacial interactions. Given that asphalt was a highly complex multiphase system, the interactions between PU, the asphalt matrix, and aggregates were intricate, and conventional experimental methods often fail to elucidate these mechanisms at the molecular scale.

With the advancement of computer technology, molecular simulation has become an important tool for investigating the microstructure and properties of materials. Molecular dynamics (MD) simulations, by modeling atomic- and molecular-level interactions, enable in-depth exploration of the mechanisms governing the interactions among PU, asphalt, and aggregates, thereby providing more accurate and systematic theoretical support for asphalt modification [22,23]. Owing to their high computational efficiency and accuracy, molecular simulation methods could elucidate the adsorption behavior of PU in asphalt, molecular structural changes, and the formation of cross-linked networks, thus helping to better understand the modification effects of PU on asphalt performance [24,25]. At the molecular scale, simulation techniques could reveal the interaction mechanisms between PU and asphalt, thereby clarifying the modification pathways of PU. For instance, Huang et al. [26] combined experiments with molecular simulations to investigate the compatibility of PU in asphalt, demonstrating that PU improved the compactness of asphalt molecular structures and exhibited good compatibility at a dosage of 15%. Zhang et al. [27] employed molecular simulations to study the rheological and thermal properties of thermoplastic polyurethane (TPU)-modified asphalt, and found that TPU significantly enhanced high-temperature performance, reduced the glass transition temperature (T_g) with increasing TPU content, and decreased the free volume fraction of asphalt, thereby improving thermal stability. Gao et al. [13] conducted a multiscale MD study on bio-based PU-modified asphalt (Bio-PUMA) and revealed good compatibility along with improved high-temperature stability and crack resistance. Although molecular simulation has proven to be a powerful tool for studying PU modification mechanisms, current research primarily emphasizes PU-asphalt compatibility and thermodynamic properties. Therefore, systematic investigations into the modification mechanisms of PU, particularly the influence of PU dosage on

asphalt–aggregate adhesion, were of significant practical importance for advancing the application of PU in asphalt modification.

In summary, this study prepared polyurethane-modified asphalts with different dosages and investigated their rheological behaviors before and after aging through rheological tests and MD simulations. The high- and low-temperature rheological properties were evaluated in combination with MD simulations to elucidate the interaction mechanisms of PU within the asphalt matrix, its effects on mechanical performance, and its interfacial adhesion with aggregates. The findings provide new insights into the application of PU-modified asphalt and the development of high-performance pavement materials.

2. Materials and Test Methods

2.1. Materials and Preparation Process

The raw materials used in this study included hydroxyl-terminated polybutadiene (HTPB), isophorone diisocyanate (IPDI), 1,4-butanediol (BDO), and 70# base asphalt. The technical specifications of the 70# base asphalt were listed in Table 1. Polyurethane-modified asphalt (PUA) was synthesized via the prepolymer method [28,29], as illustrated in Figure 1. In brief, HTPB and IPDI were mixed at 110 °C and stirred using a high-speed shear mixer at 400 rpm for 2.5 h. BDO was then added and sheared for an additional 0.5 h. The resulting prepolymer was incorporated into asphalt preheated to 150 °C and stirred at 800 rpm for 1 h, followed by curing in an oven at 150 °C for 8 h to obtain the final polyurethane-modified asphalt. During preparation, the mass ratio of HTPB, IPDI, and BDO was 1:3:2. In this study, PU contents of 10%, 20%, and 30% by mass in the base asphalt were investigated, corresponding to PU-10, PU-20, and PU-30, respectively.

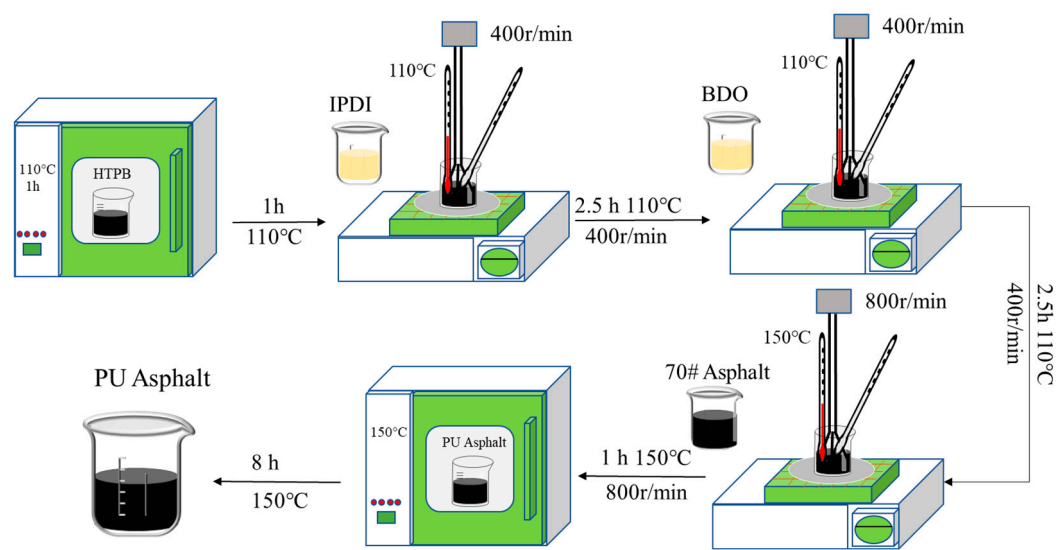


Figure 1. Synthesis method of polyurethane modified asphalt.

Table 1. 70 # matrix asphalt index.

Technology index	Technical requirement	Detect method	Test value
Needle penetration (30°C) / (0.1mm)	60~80	T0604	71
Ductility (10°C) / cm	≥20	T0605	79.4
Softening point / °C	≥46	T0606	47.3
Density (15°C) / (g/cm³)	-	T0603	1.006
Dynamic viscosity (60°C) / (Pa·s)	180~240	T0620	213

2.2. Degradation Testing

To investigate the aging behavior of PUA, samples with different aging degrees were prepared using short-term rolling thin film oven test (RTFOT), pressure aging vessel (PAV), and ultraviolet (UV) aging to simulate the service-induced aging processes. The RTFOT test was conducted following the “JTG E20-2011” standard. The aging conditions were set at $163 \pm 1\text{ }^{\circ}\text{C}$ with a rotor speed of 15 r/min for 85 min. For UV aging, a custom-made ultraviolet aging chamber was employed to perform accelerated indoor UV aging on PUA samples after RTFOT treatment. Specifically, 30 g of RTFOT-aged asphalt was placed in an aging pan with a diameter of 140 mm and subjected to UV exposure at $60\text{ }^{\circ}\text{C}$ with an intensity of 75 mW/cm^2 for 168 h. The PAV aging test was conducted on RTFOT-aged asphalt at $100\text{ }^{\circ}\text{C}$ under a pressure of 2.1 MPa for 15 h to simulate long-term aging.

2.3. Testing and Characterization

To determine the changes in the four components of asphalt before and after aging, four-component analyses were performed on PUA and 70# base asphalt. Following the JTG E20-2011 standard, n-heptane and toluene were used to separate asphalt into saturates, aromatics, resins, and asphaltenes, and their respective mass fractions were determined.

To evaluate the performance changes of PUA before and after aging, temperature sweep tests were conducted using a dynamic shear rheometer (DSR) on both PUA and 70# base asphalt in the temperature range of $40\text{--}82\text{ }^{\circ}\text{C}$, according to JTG E20 T0628 and JTG E20 T0627 standards. Low-temperature bending beam rheometer (BBR) tests were performed on PUA at $-12\text{ }^{\circ}\text{C}$ and $-18\text{ }^{\circ}\text{C}$ to assess its low-temperature rheological behavior.

3. Molecular Dynamics Simulation

3.1. Molecular Model Construction

In this research, the 12-molecule asphalt model proposed by Li et al. [30] was selected. Based on the synthesis principles and material ratios of PU, the molecular structure of PU was constructed using the “Build Polymers” module. Considering the thermo-oxidative aging characteristics of both asphalt and PU, molecular structures of aged asphalt were also developed, as illustrated in Figure 2. To ensure that the constructed molecular models corresponded to real materials, the four-component contents of unaged and aged asphalt samples were measured and were presented in Table 2. Using these four-component experimental results, the number of each of the 12 molecules in the asphalt model was determined, and the PU content was set according to the intended dosage; the calculation results were summarized in Table 3. The four-component composition of the asphalt molecular model closely matched the experimental values, indicating that the constructed asphalt molecular model accurately represents the four-component distribution [31,32].

Table 2. Four-Component Composition of Asphalt Molecular Model and Experimental Samples.

Type asphalt	Mass ratio			
	Asphaltene	Saturates	Aromatics	Colloid
Virgin	14.61%	16.14%	41.97%	27.28%
RTFOT aged	16.27%	11.55%	43.53%	28.65%
UV aged	23.69%	10.59%	34.38%	31.34%
PAV aged	24.99%	11.54%	30.54%	32.93%

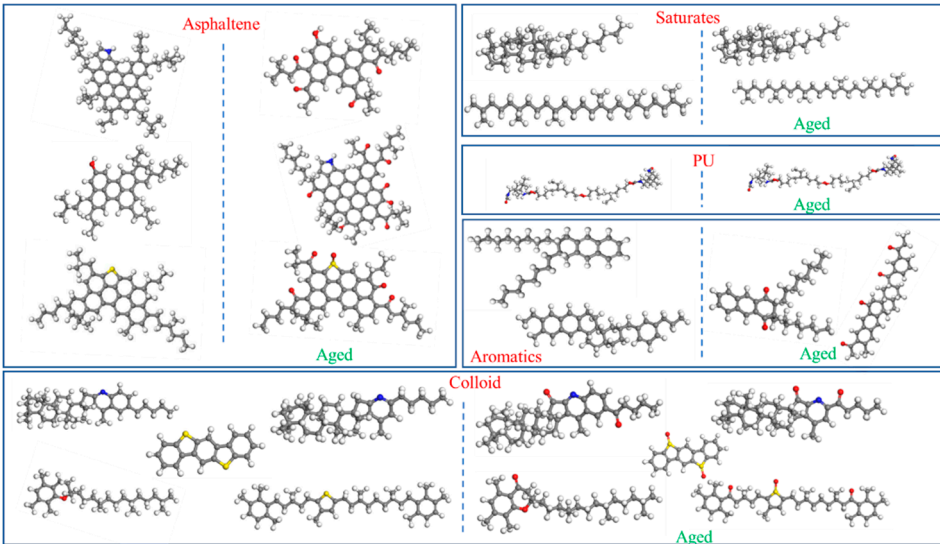


Figure 2. Molecular structure of pitch 12 and polyurethane.

Table 3. Number of asphalt molecules in different models.

Compone nt	Molecul e	Virgin		RTFOT		UV		PAV	
		Number s	Ratio%	Number s	Ratio%	Number s	Ratio%	Numbers	Ratio %
Asphalten e	Asp-1	3		3		3		4	
	Asp-2	2	14.03	2	16.19	4	23.43	6	25.11
	Asp-3	3		4		5		5	
Saturates	Hopane	9	16.12	6	11.61	6	10.66	8	11.29
	Squalene	5		5		5		4	
Aromatic	PHPN	18	42.17	18	43.85	15	34.18	14	30.72
	DOCHN	21		22		19		18	
Colloid	Colloid-1	3		4		5		5	
	Colloid-2	18		16		16		19	
	Colloid-3	1	27.68	2	28.36	3	31.73	4	32.87
	Colloid-4	2		3		4		4	
	Colloid-5	2		2		4		5	
Modifier	PU	0/2/4/6	— —	0/2/4/6	— —	0/2/4/6	— —	0/2/4/6	— —

Based on the molecular ratios presented in Table 3, molecular models of base asphalt and polyurethane-modified asphalt were constructed, with the initial model density set to 0.1 g/cm³. Due to the presence of numerous unrealistic structures in the initial models, thorough optimization and relaxation were performed, including 100,000 steps of geometry optimization, 500 ps of molecular dynamics simulation under the NVT ensemble at 298 K, five annealing cycles in the temperature range of 298–598 K, and finally 300 ps of molecular dynamics under the NPT ensemble (298 K, 1 atm), allowing the molecules to fully mix and reach a stable configuration. Throughout these procedures, the COMPASS II force field, widely used for simulating the thermodynamic properties of various polymers, was employed. Electrostatic and van der Waals interactions were treated using the Ewald method and atom-based summation, respectively. The final stabilized molecular models of base asphalt and PU-modified asphalt were shown in Figure 4.

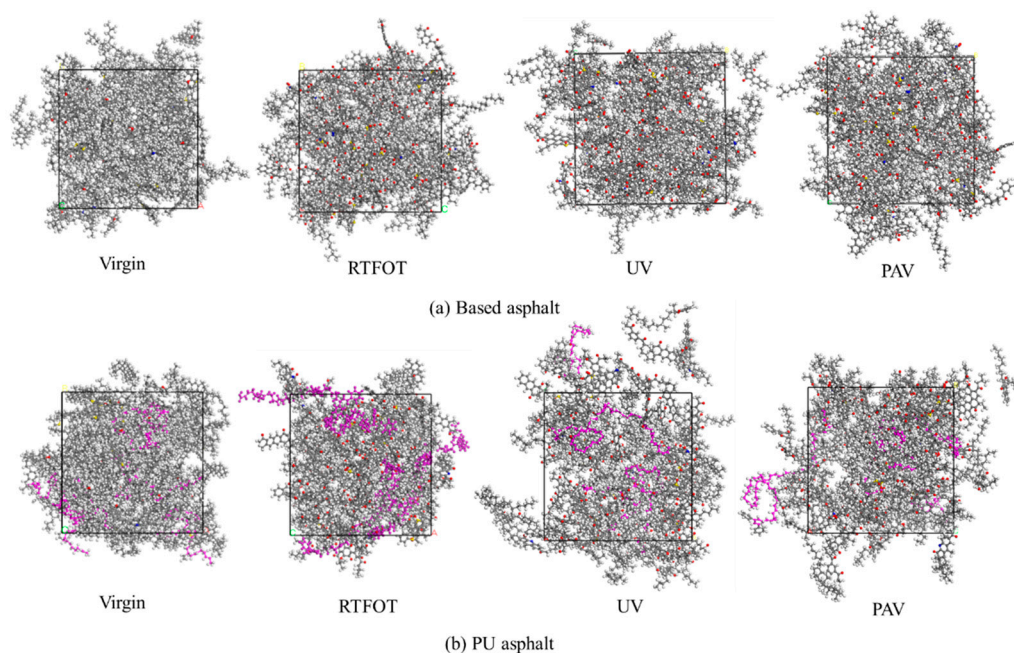


Figure 4. Asphalt molecular model.

In this research SiO_2 was selected as the representative aggregate mineral, with lattice parameters of $a=b=4.90996 \text{ \AA}$, $c=5.402 \text{ \AA}$, $\alpha=\beta=90^\circ$, and $\gamma=120^\circ$. The lattice angles were converted to 90° orthogonal crystal systems through the transformation of the unit cell, and the crystal was then cleaved along the $(0,0,1)$ plane of the SiO_2 unit cell [33,34] to construct a supercell model with three-dimensional periodic boundary conditions. The asphalt-aggregate interface model was built by stacking asphalt onto the aggregate surface, with a 70 \AA vacuum layer added to eliminate interference from periodic images. The interface model underwent 10,000 steps of geometry optimization, followed by 300 ps of molecular dynamics simulation under the NVT ensemble at 298 K, allowing full adsorption of asphalt onto the aggregate surface. The final asphalt-aggregate model as shown in Figure 5.

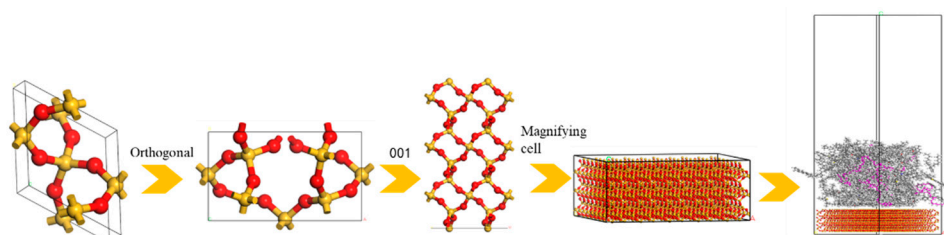


Figure 5. Polyurethane PU modified asphalt-aggregate interface model.

3.2. Analysis Method

3.2.1. Radial Distribution Function

Asphalt was an amorphous material, and different asphalt components and polyurethane modifiers exhibit distinct aggregation behaviors in a blended system due to their individual physical properties and structures. The radial distribution function (RDF) describes the ratio of the local density around a reference particle to the average density of the system and could be used to characterize molecular distribution and aggregation. The RDF $g(r)$ represents the probability of finding another particle at a distance r from a reference particle and could be calculated using Eq.1. Therefore, the distribution characteristics of asphalt molecules and polyurethane before and after aging were analyzed through the RDF curves of the respective components.

$$g(r) = \lim_{dr \rightarrow 0} \frac{dN / 4\pi r^2 dr}{N / V} \quad (1)$$

Where dN is the number of reference particles, N is the total number of particles in the system, and V is the total volume of the system.

3.2.2. Fractional Free Volume

Free volume refers to the volume not occupied by molecules. The presence of free volume allows molecules to rotate and migrate freely. Using the Connolly surface method, the free volume could be calculated, and the fractional free volume (FFV) can be determined using Eq. 2 and 3.

$$FFV = \frac{V_{free}}{V} \quad (2)$$

$$FFV = \frac{V - 1.3V_{vdw}}{V} \quad (3)$$

Where V is total volume of the model; V_{free} is free volume; V_{vdw} is Van der Waals volume.

3.2.3. Mechanical Property

In molecular simulations, the application of stress could alter the relative positions of molecules within the system. To model the mechanical response of PU asphalt as a pavement material at the molecular scale during service, the variations in mechanical properties before and after aging were investigated using Young's modulus (E), bulk modulus (K), shear modulus (G), and Poisson's ratio (ν). In this analysis, the material was assumed to be isotropic, and the stress-strain state was characterized using the Lamé constants, λ and μ .

$$\nu = \frac{\lambda}{2(\lambda + \mu)} \quad (4)$$

$$E = \frac{\mu(3\lambda + 2\mu)}{\lambda + \mu} \quad (5)$$

$$K = \lambda + \frac{2}{3}\mu \quad (6)$$

$$G = \mu \quad (7)$$

3.2.4. Interface Adhesion Properties

To evaluate the interfacial adhesion performance between PU asphalt and aggregates, the work of adhesion was employed. At the asphalt-aggregate interface, the energy required to completely separate the two phases was defined as the binding energy, and the adhesion energy between asphalt and aggregate was calculated using Eq. 8. To quantitatively assess adhesion differences while eliminating the influence of interface size, the work of adhesion was used as an indicator of interfacial bonding performance. A higher work of adhesion corresponds to stronger adhesion between asphalt and aggregate, as expressed in Eq. 9.

$$E_{int} = E_a + E_b - E_{a-b} \quad (8)$$

$$W = \frac{E_{int}}{A} \quad (9)$$

Where E_{a-b} is represents the total energy of the interface system; E_a is the energy of the asphalt; E_b is the energy of the aggregate; E_{int} denotes the binding energy at the asphalt-aggregate interface; and A is the interfacial contact area between asphalt and aggregate.

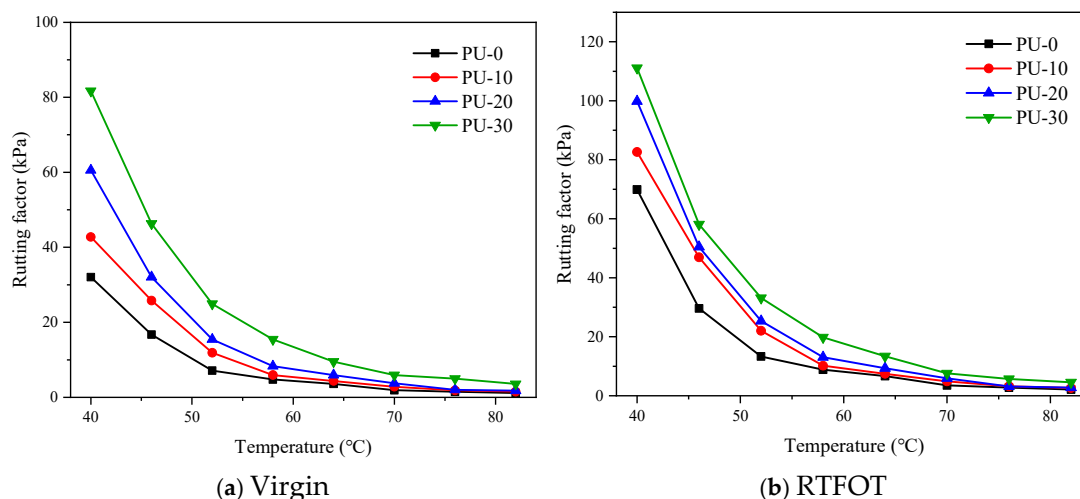
4. Results and Discussion

4.1. Evaluation of Rheological Properties

4.1.1. Analysis of High Temperature Anti-Rutting Performance

The rutting factor, an important indicator for evaluating asphalt performance established under the SHRP program, reflects the high-temperature rheological behavior of asphalt binders. Under the same high-temperature conditions, a higher rutting factor indicates a stronger resistance of the asphalt material to high-temperature deformation. The rutting factor of 70# base asphalt and PU-modified asphalt before and after aging was shown in Figure 6. The results indicate that, at the same temperature, the rutting factor increases significantly with increasing PU content. This suggests that the addition of PU not only acts as a filler, reducing the viscous flow of asphalt, but also forms a stable network structure within the asphalt matrix, adsorbing and immobilizing lighter components such as aromatics, thereby hindering the mobility of large molecular chains at high temperatures and overall enhancing the material's resistance to permanent deformation.

Furthermore, after UV aging, the rutting factor of asphalt with different PU dosages increased significantly, reflecting the hardening of the asphalt matrix caused by aging. A further comparison reveals that as the degree of asphalt aging increases, its high-temperature permanent deformation resistance gradually decreases, evidenced by the continuous rise in the rutting factor. This effect is more pronounced in base asphalt, indicating that it was more prone to plastic flow and structural failure under high-temperature loading, accelerating rut formation. This phenomenon was closely related to the volatilization of light components and the oxidative hardening of resins and asphaltenes during aging, leading to a gradual loss of viscoelastic balance in the material. In contrast, although PU-modified asphalt was also affected by aging, the increase in its rutting factor was relatively smaller, suggesting that PU modification could partially mitigate the deterioration of high-temperature performance caused by aging. The underlying mechanism may be attributed to the stability of the PU cross-linked structure, which effectively delays oxidative reactions in the asphalt matrix and enhances elasticity and toughness, thereby improving resistance to permanent deformation. These results indicate that PU modification not only enhances the high-temperature stability of asphalt but also reduces its sensitivity to aging.



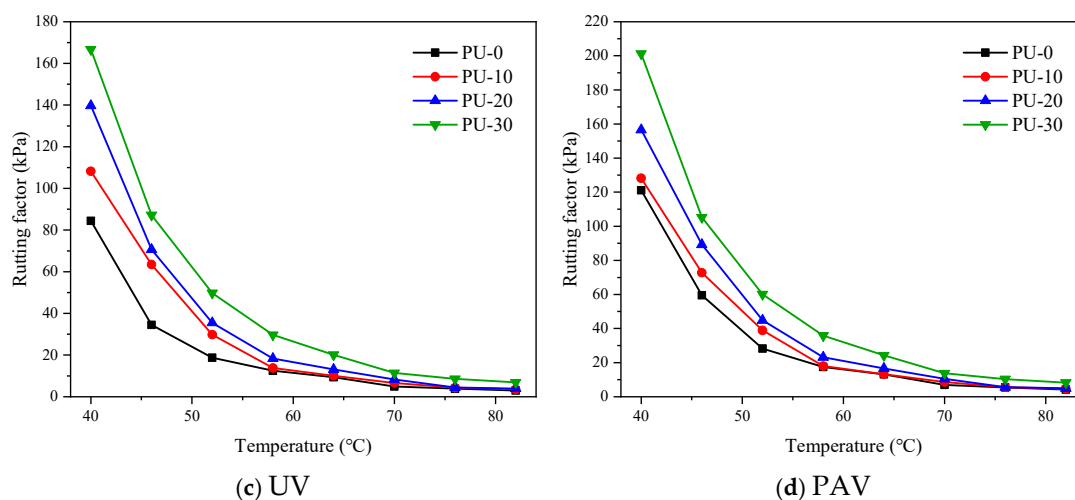


Figure 6. Rutting factor test results.

4.1.2. Analysis of Low Temperature Rheological Properties

To systematically evaluate the low-temperature flexibility and stress-relaxation capability of PU-modified asphalt, BBR tests were conducted to obtain the stiffness modulus (S) and creep rate (m), which were key indicators for characterizing asphalt low-temperature performance. According to standard requirements, the S value should be less than 300 MPa, and the m value should be greater than 0.3. A lower S indicates stronger deformation capacity and better flexibility under the same stress, whereas a higher m signifies enhanced stress-relaxation ability, effectively mitigating low-temperature shrinkage stress concentration and reducing the risk of cracking. The test results were shown in Figure 7 and Figure 8. The data demonstrate that as temperature increases, the stiffness modulus of asphalt decreases significantly, while the creep rate increases, reflecting that molecular chain mobility was higher at elevated temperatures, leading to improved flexibility. Conversely, at low temperatures, molecular motion was restricted, causing asphalt to harden and become brittle, increasing the likelihood of fracture.

Comparative results indicate that PU addition effectively improves the low-temperature performance of asphalt. Specifically, PU-modified asphalt exhibits a markedly lower stiffness modulus and a significantly higher creep rate than base asphalt, suggesting that PU modification enhances material flexibility and stress-relaxation capability, thereby mitigating low-temperature cracking. This improvement may be attributed to PU adsorbing part of the resin components and forming a stable cross-linked network within the asphalt matrix, which strengthens intermolecular interactions and enhances resistance to low-temperature deformation. Under aging conditions, the stiffness modulus of base asphalt generally exceeds 300 MPa, failing to meet the standard requirements. In contrast, PU-modified asphalt maintains its stiffness modulus within the standard limit even after aging, demonstrating superior low-temperature crack resistance and longer service life.

Further analysis of different aging methods shows that RTFOT short-term aging only causes a slight increase in stiffness modulus, whereas UV and PAV aging result in substantial increases, with PAV aging exhibiting the most pronounced effect. Base asphalt subjected to UV and PAV aging shows stiffness moduli exceeding 300 MPa, indicating significant loss of low-temperature flexibility and a high susceptibility to cracking. In comparison, PU-modified asphalt under the same aging conditions exhibits a markedly smaller increase in stiffness modulus, remaining below 300 MPa, demonstrating excellent anti-aging performance. These results suggest that PU incorporation has a significant advantage in delaying low-temperature performance degradation.

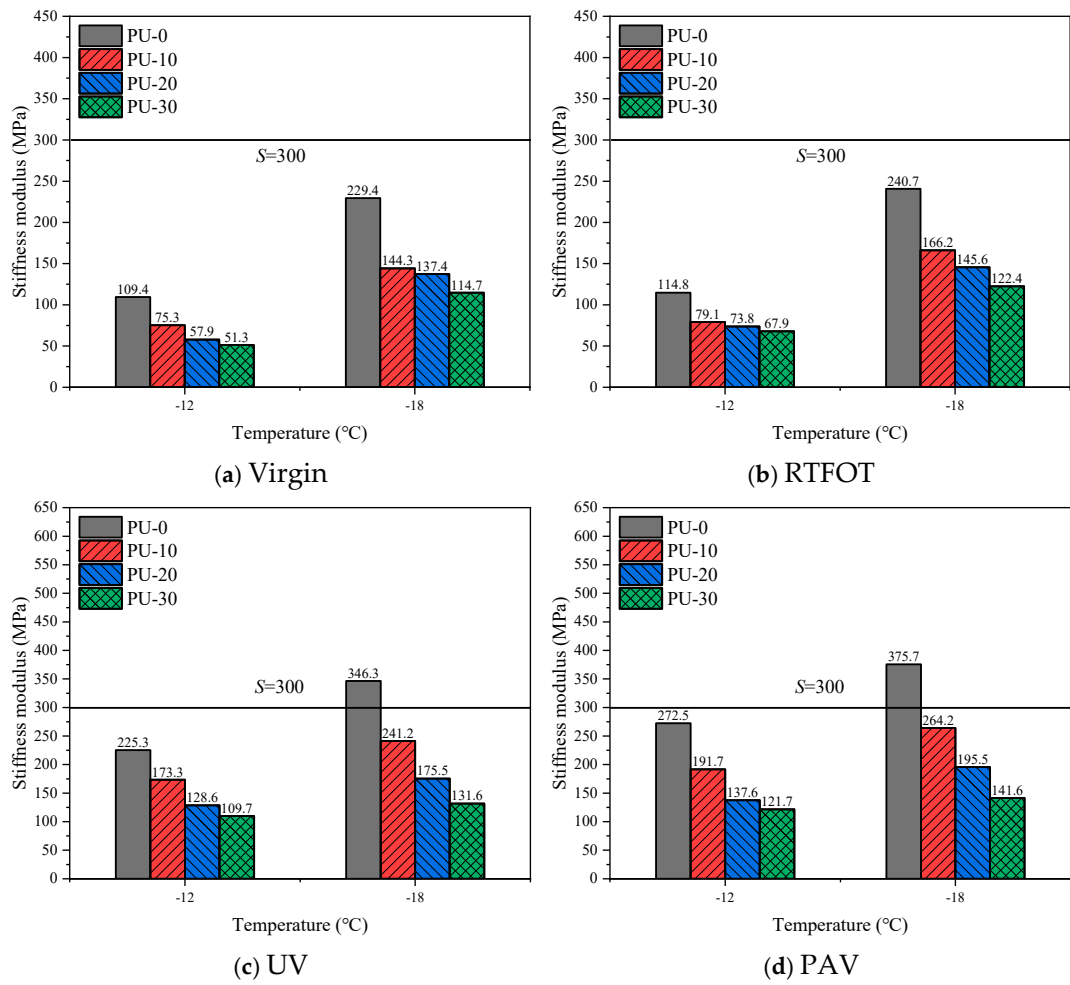
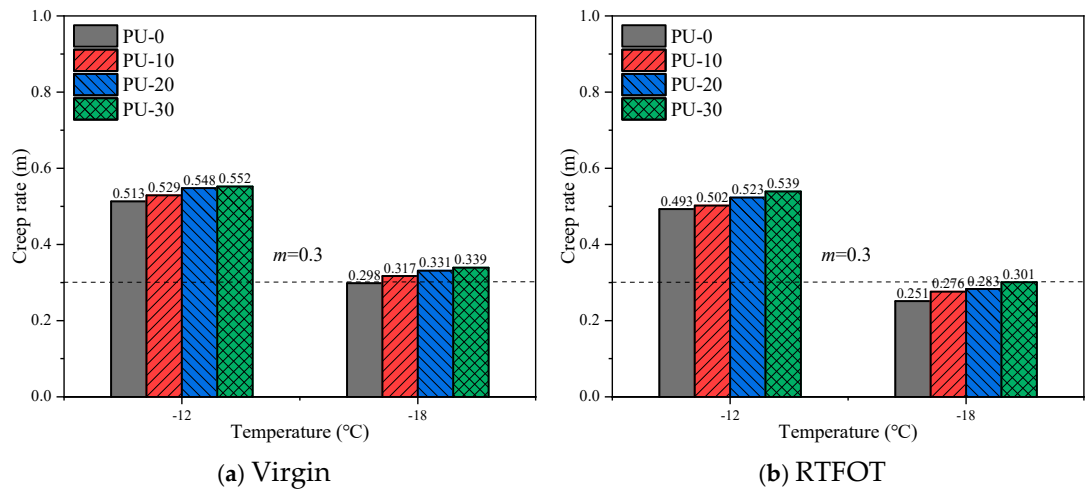


Figure 7. Stiffness modulus test results.



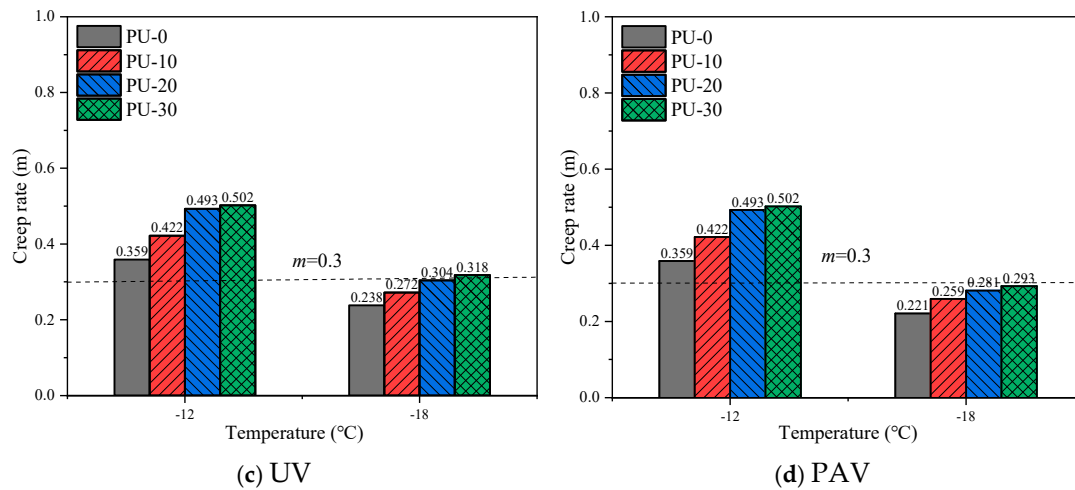


Figure 8. Creep rate test results.

4.2. Analysis of Molecular Dynamics Results

4.2.1. RDF Analysis

To further evaluate the distribution characteristics of PU within the asphalt matrix, Figure 9a presents the RDF of PU in the asphalt molecular model, while Figure 9b illustrates the RDF between PU and different asphalt components for PU-modified asphalt with a 10% PU content. As shown, the distance between PU and light components such as saturates and aromatics was approximately 1.3 Å, indicating that PU could maintain close proximity to these light fractions after incorporation into asphalt. This proximity facilitates the formation of a certain cross-linked network, which adsorbs and immobilizes more light components, thereby reducing their migration and volatilization at high temperatures and enhancing the overall stability and anti-aging performance of asphalt.

Additionally, the RDF curves of PU itself show that at 10% and 20% PU content, the peak positions were nearly identical, suggesting that PU was relatively uniformly dispersed within the asphalt matrix without significant aggregation in this range. However, when the PU content increases to 30%, a sharp change in the RDF peak was observed, indicating pronounced self-aggregation of PU molecules. Such excessive aggregation may disrupt the original colloidal stability of asphalt, leading to local phase separation and segregation, which could weaken the mechanical properties and service stability of the material. Therefore, when using PU to modify asphalt, the PU content should be kept below 30% to balance network formation and dispersion stability, avoiding the adverse effects associated with excessive PU addition.

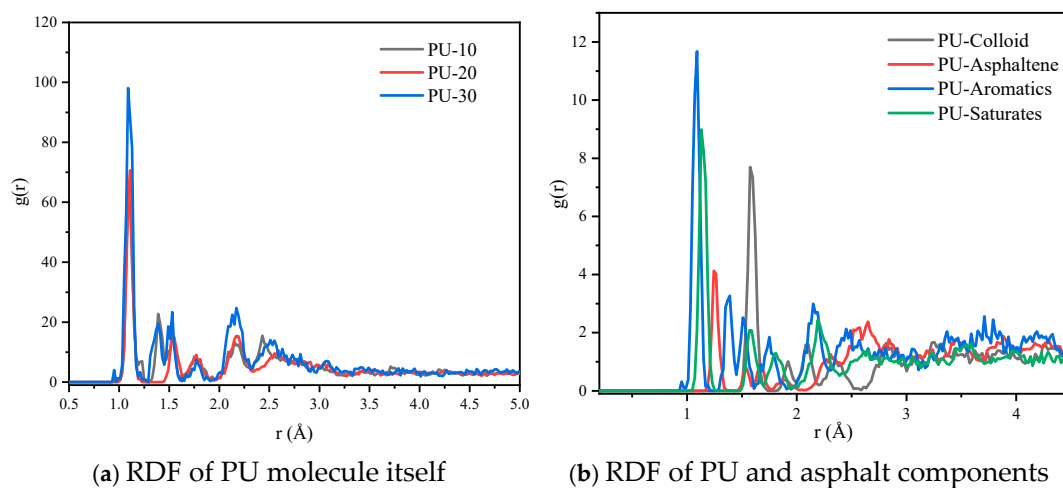


Figure 9. RDF curve.

4.2.2. Fractional Free Volume

In molecular dynamics simulations, the *FFV* was an important parameter for evaluating the rheological performance of asphalt materials, reflecting the size of unoccupied spaces between molecules and closely relating to molecular mobility, system viscosity, and flowability. In this research, the *FFV* distribution of PU-modified asphalt models with different PU contents before and after aging was calculated (Figure 10), and the results were summarized in Table 4. The data indicate that before aging, the addition of PU significantly reduces the *FFV* of the asphalt matrix, and *FFV* decreases progressively with increasing PU content. This suggests that PU could adsorb and immobilize light components while forming a stable cross-linked network, reducing inter-molecular voids and mobility regions, and leading to a more compact system structure. The restricted molecular thermal motion in the presence of long-chain PU increases the viscosity of the modified asphalt compared to base asphalt, enhancing its resistance to deformation under external loads and exhibiting superior high-temperature rutting resistance.

As aging progresses, the overall *FFV* decreases, reflecting the oxidation and volatilization of light components and the relative increase of resins and asphaltenes, which result in tighter molecular chain packing. Notably, the decrease in *FFV* for PU-modified asphalt under the same aging conditions was significantly smaller than that of base asphalt, indicating that PU effectively preserves molecular mobility and flexibility during aging, thereby mitigating high-temperature performance degradation. In other words, the PU cross-linked network not only densifies the initial structure but also acts as a stabilizer under aging conditions, suppressing excessive loss of light components and over-hardening of molecular structures, thereby markedly enhancing asphalt’s anti-aging performance. These results demonstrate that PU-modified asphalt has strong potential for extending service life while maintaining high-temperature rheological properties.

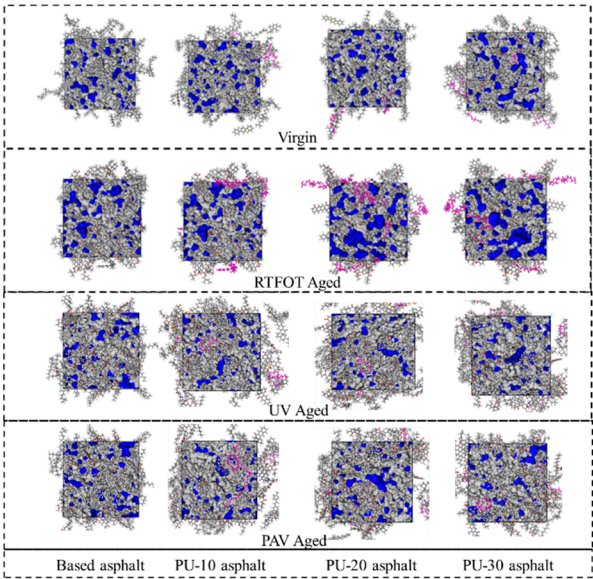


Figure 10. Free volume distribution map.

Table 4. Free volume fraction of modified asphalt before and after aging.

Type	FFV (%)			
	Virgin	RTFOT Aged	UV Aged	PAV Aged
PU-0	24.86	23.41	19.72	18.61
PU-10	22.73	20.63	17.26	16.94
PU-20	21.07	19.02	17.03	16.54
PU-30	20.68	17.93	16.74	16.19

4.2.3. Mechanical Property

To evaluate the mechanical properties of PU-modified asphalt, stable molecular models of different systems were used to simulate mechanical behavior, and the mechanical parameters of base asphalt and PU-modified asphalt with varying PU contents were calculated, as shown in Figure 11. Figure 12 illustrates that with increasing PU content, all mechanical properties of the modified asphalt exhibit an upward trend, indicating that the modulus increases with PU addition and significantly enhances the material’s resistance to deformation under external loads. This improvement was primarily attributed to the long-chain structure of PU, which forms a cross-linked network within the asphalt and adsorbs part of the light components, thereby increasing system viscosity and structural density and enhancing mechanical strength and deformation resistance.

As aging progresses, the mechanical properties of all systems decrease to varying degrees; however, the degradation of PU-modified asphalt was significantly less than that of base asphalt. This suggests that the PU cross-linked network not only reinforces mechanical strength in the unaged state but also acts as a stabilizer during aging, effectively mitigating the loss of light components and excessive hardening of molecular structures, thereby markedly enhancing the asphalt’s anti-aging performance.

With further PU addition up to 20%, mechanical properties continue to improve; however, when the PU content reaches 30%, the rate of performance enhancement diminishes significantly. This was likely due to excessive PU causing local aggregation or phase separation, disrupting the homogeneity of the asphalt colloid and limiting further improvement of mechanical performance. Therefore, in modification design, the PU content should be carefully optimized to balance mechanical performance and system stability. Overall, analysis indicates that a PU content of approximately 20% provides a favorable combination of enhanced mechanical properties while avoiding colloidal segregation issues.

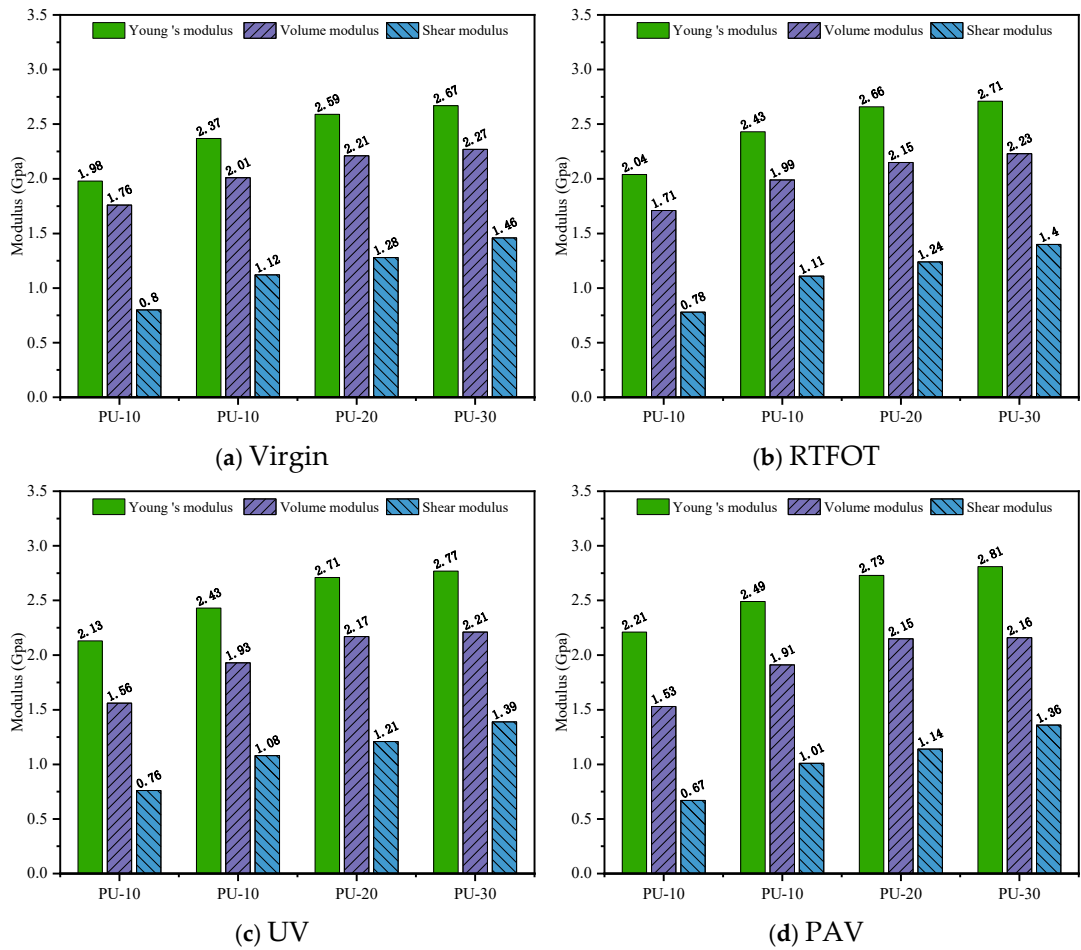


Figure 11. Asphalt mechanical properties index.

4.3. Interface Adhesion Properties

The mechanical strength of asphalt mixtures largely depends on the effective adhesion between asphalt and aggregate, as interfacial adhesion directly influences the overall mechanical performance of the mixture. To investigate the effect of PU incorporation on asphalt–aggregate interfacial adhesion, molecular dynamics simulations were conducted for interfaces with varying PU contents. In the interface model, the energy required to separate asphalt from the aggregate was defined as the work of adhesion, which directly reflects the asphalt–aggregate bonding strength. Higher adhesion energy indicates a more stable interfacial connection. In this study, the average adhesion energy was calculated over all frames after the interface model reached a stable adsorption conformation, providing the adhesion energies for asphalt in contact with two types of aggregates, as shown in Figure 12.

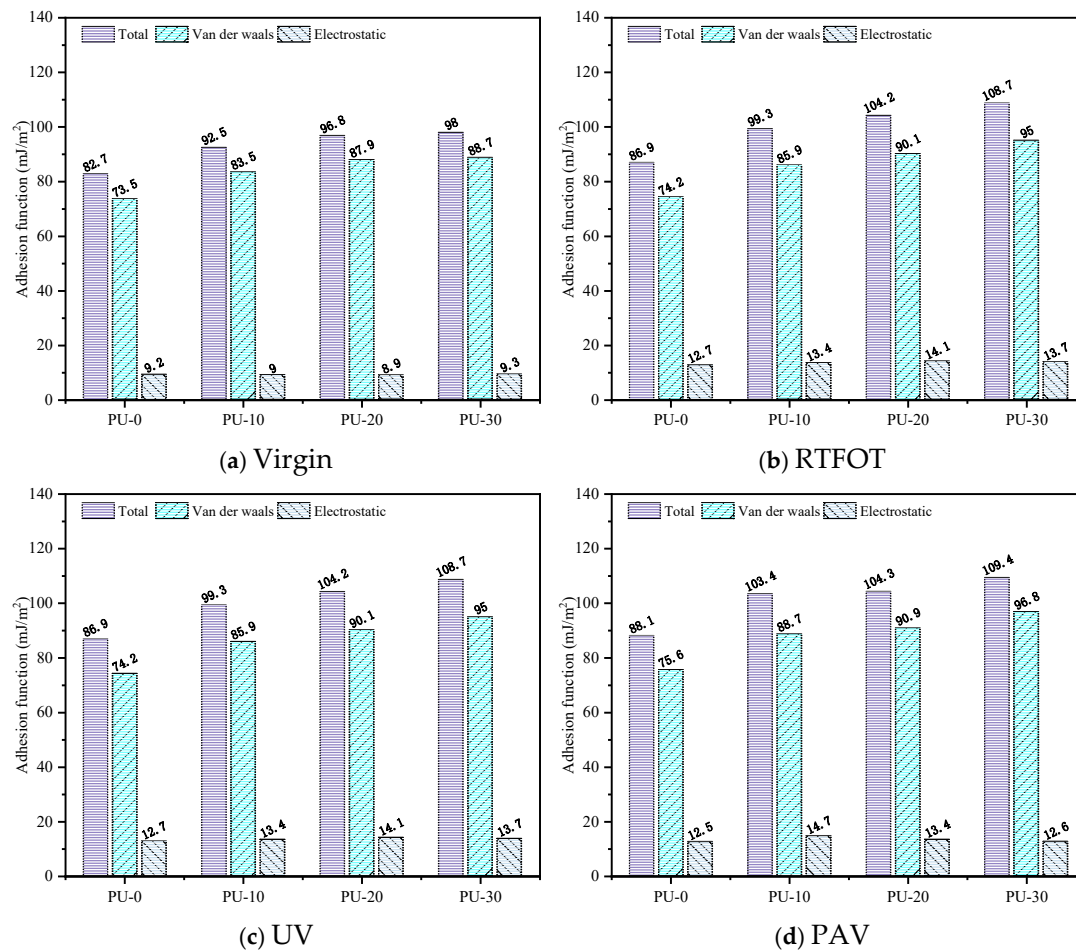


Figure 12. Adhesion work of PU modified asphalt and aggregate.

The analysis indicates that the adhesion energy at the asphalt–aggregate interface was mainly derived from non-bonded interactions, with van der Waals forces being dominant and electrostatic interactions secondary, suggesting that the interfacial adhesion was primarily physical in nature. The incorporation of PU enhances intermolecular interactions and improves asphalt–aggregate interfacial contact, leading to a significant increase in adhesion energy, which highlights the role of PU in optimizing interfacial bonding and improving the mechanical performance of asphalt mixtures. However, when the PU content increases from 20% to 30%, the increment in adhesion energy diminishes. This may be attributed to excessive PU causing partial molecular aggregation or phase separation, limiting further improvement of interfacial stability. The main contributor to the increase in adhesion energy was the enhanced van der Waals interaction, likely resulting from PU restricting asphalt molecular mobility and diffusion, increasing system viscosity, and facilitating stronger asphalt attachment to the aggregate surface.

5. Conclusion

This research employed laboratory experiments and molecular simulation techniques to investigate the modification mechanisms of PU in asphalt at micro- and molecular scales, and to examine the effect of PU on asphalt–aggregate interfacial adhesion. The main conclusions were as follows:

(1) Incorporation of PU into asphalt significantly improves rutting resistance, low-temperature flexibility, and stress relaxation capacity. Although ultraviolet aging leads to some decline in rheological performance, the aged PU-modified asphalt still exhibits superior properties compared to base 70# asphalt. This improvement was primarily attributed to the PU network structure mitigating the performance degradation caused by the oxidation and polymerization of light components into higher asphaltene content during aging.

(2) PU adsorbs light components in asphalt and forms a cross-linked network, resulting in a substantial reduction of free volume in the molecular model and a decrease in molecular mobility, thereby enhancing the asphalt's resistance to external loads. After aging, the reduction in free volume fraction of PU-modified asphalt was significantly smaller than that of base asphalt, indicating that PU effectively delays molecular structure hardening and enhances asphalt's anti-aging performance.

(3) The mechanical properties, rutting factor, and stiffness modulus of PU-modified asphalt increase with PU content. However, at a PU content of 30%, molecular models indicate partial PU aggregation or phase separation, leading to abnormally high RDF peaks and reduced system stability. Therefore, considering both performance and stability, the optimal PU content in asphalt was approximately 20%.

(4) Asphalt–aggregate interfacial adhesion was primarily governed by physical interactions, with van der Waals forces being dominant and electrostatic interactions secondary. The addition of PU significantly enhances the adhesion energy between asphalt and aggregate, strengthens interfacial bonding, and maintains high adhesion even after aging, thereby further improving the mechanical stability and durability of asphalt mixtures.

Acknowledgement: The research was supported by the National Natural Science Foundation of China (Grant No. 52508501); the Natural Science Foundation of Hunan Providence (Grant No. 2025JJ60343); the Scientific Research Project of the Education Department of Hunan Province (Grant No. 24B0419).

Declaration of Interest: The authors declare that they have no conflict of interest.

Reference

1. Liu, F, Hu, Z, Wang, B, et al. Molecular dynamics and experimental investigation on the mechanism and properties of nano-silica/graphene composite-modified asphalt. *Construction and Building Materials*, 2025. **493**: p. 143309. DOI: <https://doi.org/10.1016/j.conbuildmat.2025.143309>.
2. Xiong, L, Liu, K, Kadhim, H A, et al. Comparative analysis of the fatigue characterisation of natural rock asphalt/SBS composite modified asphalt binders using time sweep test and linear amplitude sweep test. *Construction and Building Materials*, 2025. **494**: p. 143315. DOI: <https://doi.org/10.1016/j.conbuildmat.2025.143315>.
3. Guo, M, Xie, X, Gou, J, et al. Heterogeneous diffusion between recycled crumb rubber modified asphalt and virgin asphalt binders: Rheological methods and microstructure characterization. *Construction and Building Materials*, 2025. **494**: p. 143392. DOI: <https://doi.org/10.1016/j.conbuildmat.2025.143392>.
4. Jin, X, Li, D, Gong, M, et al. Study on the intrinsic mechanism and adhesion performance mapping of block copolymer modified polyurethane prepolymer (M-PPU) modified asphalt. *Construction and Building Materials*, 2025. **494**: p. 143368. DOI: <https://doi.org/10.1016/j.conbuildmat.2025.143368>.
5. Wu, W, Huang, M, Li, C, et al. Effect of waste cooking oil on ethylene vinyl acetate modified asphalt based on multiscale study. *Construction and Building Materials*, 2025. **492**: p. 142689. DOI: <https://doi.org/10.1016/j.conbuildmat.2025.142689>.

6. Ban, X, Ji, J, You, Z, et al. Synthesis of castor oil-based polyurethane (PU) containing different disulfide contents and self-healing properties of the PU modified asphalt. *Construction and Building Materials*, 2025. **491**: p. 142658. DOI: <https://doi.org/10.1016/j.conbuildmat.2025.142658>.
7. Cao, Z, Hao, Q, Xu, S, et al. Preparation and performance evaluation of bio-based polyurethane modified asphalt binders: Towards greener and more sustainable asphalt modifier. *Construction and Building Materials*, 2025. **476**: p. 141209. DOI: <https://doi.org/10.1016/j.conbuildmat.2025.141209>.
8. Xia, W, Xu, Z, and Xu, T. Self-healing behaviors and its effectiveness evaluations of fiber reinforced shape memory polyurethane/SBS modified asphalt mortar. *Case Studies in Construction Materials*, 2023. **18**: p. e01784. DOI: <https://doi.org/10.1016/j.cscm.2022.e01784>.
9. Huang, G, Yang, T, He, Z, et al. Polyurethane as a modifier for road asphalt: A literature review. *Construction and Building Materials*, 2022. **356**: p. 129058. DOI: <https://doi.org/10.1016/j.conbuildmat.2022.129058>.
10. Min, Z, Chen, W, Yang, H, et al. Optimization of preparation process and pavement performance evaluation of polyurethane-modified epoxy asphalt mixtures. *Construction and Building Materials*, 2025. **486**: p. 141881. DOI: <https://doi.org/10.1016/j.conbuildmat.2025.141881>.
11. Lu, J, Xu, S, Li, C, et al. The latest research progress of polyurethane modified asphalt binder: synthesis, characterization, and applications. *International Journal of Adhesion and Adhesives*, 2025. **140**: p. 104035. DOI: <https://doi.org/10.1016/j.ijadhadh.2025.104035>.
12. Motamedi, M, Shafabakhsh, G, and Azadi, M. Evaluation of fatigue and rutting properties of asphalt binder and mastic modified by synthesized polyurethane. *Journal of Traffic and Transportation Engineering (English Edition)*, 2021. **8**(6): p. 1036-1048. DOI: <https://doi.org/10.1016/j.jtte.2020.05.006>.
13. Gao, J, Guo, G, Wang, H, et al. Multiscale characterization of bio-based polyurethane modified asphalt: Macro-micro experiments and molecular dynamics simulations. *Construction and Building Materials*, 2025. **491**: p. 142699. DOI: <https://doi.org/10.1016/j.conbuildmat.2025.142699>.
14. Zhang, M, Xiong, K, Zhang, J, et al. Evaluation of the rheological properties and aging resistance of asphalt modified by MDI/TDI polyurethane. *Construction and Building Materials*, 2024. **411**: p. 134350. DOI: <https://doi.org/10.1016/j.conbuildmat.2023.134350>.
15. Jin, X, Guo, N, You, Z, et al. Rheological properties and micro-characteristics of polyurethane composite modified asphalt. *Construction and Building Materials*, 2020. **234**: p. 117395. DOI: <https://doi.org/10.1016/j.conbuildmat.2019.117395>.
16. Wang, H, Tang, N, and Zhang, R. Preparation and property controllability of dynamically crosslinked polyurethane modified bitumen. *Construction and Building Materials*, 2025. **491**: p. 142700. DOI: <https://doi.org/10.1016/j.conbuildmat.2025.142700>.
17. Long, K, Huang, C, Yang, Y, et al. Investigation of the rheological properties and aging performance of rock asphalt/thermoplastic polyurethane composite modified asphalt. *Construction and Building Materials*, 2025. **458**: p. 139699. DOI: <https://doi.org/10.1016/j.conbuildmat.2024.139699>.
18. Li, K, Yan, X, Wang, Y, et al. Experimental analysis and molecular dynamics simulation of anti-aging performance of weather-resistant polyurethane-modified asphalt. *Construction and Building Materials*, 2025. **458**: p. 139653. DOI: <https://doi.org/10.1016/j.conbuildmat.2024.139653>.
19. Jin, X, Li, D, Fu, H, et al. Research on fatigue self-healing of asphalts modified by thermoplastic polyurethane (TPU) with different soft segments. *Construction and Building Materials*, 2024. **420**: p. 135574. DOI: <https://doi.org/10.1016/j.conbuildmat.2024.135574>.
20. Kong, L, Wang, Z, Su, S, et al. Exploring the interplay between thermo-oxidative degradation and asphalt aging in thermoplastic polyurethane-modified asphalt: Mechanisms, properties, and performance evolution. *Construction and Building Materials*, 2024. **412**: p. 134694. DOI: <https://doi.org/10.1016/j.conbuildmat.2023.134694>.
21. Wang, S, Wei, K, Yu, J, et al. Polyurethane/aggregate interfacial adhesion characteristics and thin layer covering performance research. *Journal of Cleaner Production*, 2025. **519**: p. 145980. DOI: <https://doi.org/10.1016/j.jclepro.2025.145980>.

22. Shi, W, Wei, K, Guo, X, et al. Study on the interfacial adhesion performance of polyurethane-modified asphalt based on molecular dynamics simulation. *Applied Surface Science*, 2025. **685**: p. 162041. DOI: <https://doi.org/10.1016/j.apsusc.2024.162041>.
23. Cong, P, Liu, C, Han, Z, et al. A comprehensive review on polyurethane modified asphalt: Mechanism, characterization and prospect. *Journal of Road Engineering*, 2023. **3**(4): p. 315-335. DOI: <https://doi.org/10.1016/j.jreng.2023.10.001>.
24. Yang, F, Gong, H, Cong, L, et al. Investigating on polymerization process and interaction mechanism of thermosetting polyurethane modified asphalt. *Construction and Building Materials*, 2022. **335**: p. 127261. DOI: <https://doi.org/10.1016/j.conbuildmat.2022.127261>.
25. Yu, R, Wang, Q, Wang, W, et al. Polyurethane/graphene oxide nanocomposite and its modified asphalt binder: Preparation, properties and molecular dynamics simulation. *Materials & Design*, 2021. **209**: p. 109994. DOI: <https://doi.org/10.1016/j.matdes.2021.109994>.
26. Huang, T, Zhang, Z, Wang, L, et al. Study on the compatibility between polyurethane and asphalt based on experiment and molecular dynamics simulation. *Case Studies in Construction Materials*, 2022. **17**: p. e01424. DOI: <https://doi.org/10.1016/j.cscm.2022.e01424>.
27. Zhang, Z, Yu, X, Wang, Z, et al. MDI-PTMG-based TPU modified asphalt: Preparation, rheological properties and molecular dynamics simulation. *Fuel*, 2025. **379**: p. 133007. DOI: <https://doi.org/10.1016/j.fuel.2024.133007>.
28. Li, H, Ren, J, Zuo, X, et al. Preparation and properties of hydroxy-terminated polybutadiene polyurethane-modified asphalt. *Construction and Building Materials*, 2024. **453**: p. 138580. DOI: <https://doi.org/10.1016/j.conbuildmat.2024.138580>.
29. Wang, J, Hong, B, Wang, D, et al. Performance and modification mechanism investigation of polyurethane prepolymer system modified bitumen for 100 % reclaimed asphalt pavement (RAP) application. *Construction and Building Materials*, 2025. **462**: p. 139882. DOI: <https://doi.org/10.1016/j.conbuildmat.2025.139882>.
30. Li, D D and Greenfield, M L. Chemical compositions of improved model asphalt systems for molecular simulations. *Fuel*, 2014. **115**: p. 347-356. DOI: <https://doi.org/10.1016/j.fuel.2013.07.012>.
31. Ge, J, Yu, H, Qian, G, et al. Evaluation on the diffusion-fusion properties and interfacial mechanical behavior of virgin and aged asphalt. *Journal of Cleaner Production*, 2024. **477**: p. 143788. DOI: <https://doi.org/10.1016/j.jclepro.2024.143788>.
32. Yu, H, Ge, J, Qian, G, et al. Evaluation on the rejuvenation and diffusion characteristics of waste cooking oil on aged SBS asphalt based on molecular dynamics method. *Journal of Cleaner Production*, 2023. **406**: p. 136998. DOI: <https://doi.org/10.1016/j.jclepro.2023.136998>.
33. Ge, J, Yu, H, Qian, G, et al. Enhancement mechanism of aggregate surface roughness structure on interfacial properties of asphalt mixtures. *Construction and Building Materials*, 2024. **449**: p. 138388. DOI: <https://doi.org/10.1016/j.conbuildmat.2024.138388>.
34. Yu, H, Ge, J, Qian, G, et al. Evaluation of the interface adhesion mechanism between SBS asphalt and aggregates under UV aging through molecular dynamics. *Construction and Building Materials*, 2023. **409**: p. 133995. DOI: <https://doi.org/10.1016/j.conbuildmat.2023.133995>.

Disclaimer/Publisher's Note: The statements, opinions and data contained in all publications are solely those of the individual author(s) and contributor(s) and not of MDPI and/or the editor(s). MDPI and/or the editor(s) disclaim responsibility for any injury to people or property resulting from any ideas, methods, instructions or products referred to in the content.